

The Formation of RuO₂ Structures on *Cladosporium Cladosporioides* Hyphal and an Investigation of their Properties

Harun KAYA

Malatya Turgut Özal University, Yeşilyurt Vocational School, Yeşilyurt, Malatya, Türkiye,
harun.kaya@ozal.edu.tr

Abstract

In this study, ruthenium oxide (RuO₂) was grown on *Cladosporium Cladosporioides* hyphal using a chemical precipitation method. The morphological characteristics of the material obtained by chemical precipitation method were determined by Scanning Electron Microscope (SEM); its surface area by Brunauer-Emmett-Teller (BET) equipment and its electrochemical properties, such as charging–discharging, cyclic voltammetry (CV) and electrochemical impedance characteristics, using a Gamry 3000 potentiostat system.

Keywords: RuO₂, Fungi Hypal, Supercapacitor.

Cladosporium Cladosporioides Fungus Hifleri Üzerinde RuO₂ Yapılarının Oluşumu ve Özelliklerinin İncelenmesi

Özet

Bu çalışmada RuO₂ yüksek spesifik kapasitans değerinden dolayı *Cladosporium cladosporioides* mantar hifleri üzerinde kimyasal çöktürme yöntemiyle büyütüldü. Kimyasal çöktürme sonucunda elde edilen malzemenin morfolojik özellikleri taramalı elektro mikroskopu (SEM), yüzey alanı Brunauer–Emmett–Teller (BET) cihazı, cyclic

voltametri (CV), dolma-boşalma ve elektrokimyasal empedans spektroskopisi gibi elektrokimyasal özellikleri ise Gamry 3000 potansiyostat sistemi ile belirlendi.

Anahtar Kelimeler: RuO₂, Fungus hifleri, Süperkapasitör.

1. Introduction

Supercapacitors have attracted more attention than other energy storage devices in recent years due to their extremely fast charge–discharge rates, excellent stability, long cycle life and very high power density. These features are desirable to produce the energy many electric vehicles using new technology need. Because of their low energy density, supercapacitors are suitable for use as an energy source for short-term, energy-demanding scenarios. To increase the energy density of supercapacitors, the capacitance value needs to be increased as much as possible. In addition, the increase in the energy and power density can be achieved by extending the voltage window. For this purpose, it is very important to develop nanostructured materials for supercapacitor manufacturing. It has been found out that some metal oxides like RuO₂, IrO₂, MnO₂, NiO, Co₂O₃, Co₃O₄, SnO₂, V₂O₅ and MoO_x show high specific capacitance [1-16]. Among the transition metal oxides, ruthenium oxide is a very promising electrode material due to its high specific capacitance, high electrical conductivity, long cycle life and good electrochemical reversibility [17-21]. In the production of nanostructured materials, the use of microorganisms like fungi, bacteria and spores as substrates, due to their different surfaces and shapes, has become a separate area of research [6, 7, 22]. The use of biological structures as a substrate increases the surface area of nanostructured materials grown on them. Hyphal are especially preferred for the production of microtubes [7, 22-27]. Due to their low cost and being environmentally friendly, the production of metal oxide nanostructures on biological substrates such as fungi can be advantageous [22]. The use of biological substrates in the production of ruthenium oxide nanostructures has reduced the cost and enabled the use of ruthenium in smaller quantities. In this study, nanostructured RuO₂ microtubes were produced using fungi hyphal and their electrochemical capacitive properties were investigated.

2. Materials and Methods

The *Cladosporium cladosporioides* fungi to be used as a substrate material in supercapacitor manufacturing were obtained from the ATCC (American Type Culture Collection), and stock cultures were prepared in a laboratory environment. Fungal cultures incubated under appropriate conditions were planted in a sterilized PDB (Potato Dextrose Broth) medium in the ratio of 1 ml fungal culture /50 ml broth. This was centrifuged several times with distilled water and ethanol to remove the culture medium from the produced fungi. Five grams of $\text{RuCl}_2 \cdot x\text{H}_2\text{O}$ solution was dissolved in 200 ml of pure water and dropped onto the hyphal obtained after this washing process at a rate of 10 ml/min while stirring at 170 rpm. The fungi/ RuCl_2 suspension was again stirred at 170 rpm for 30 minutes. After this time, 100 ml of 25 mM of NH_4OH solution was dropped onto the suspension at a rate of 10 ml/min, and the solution was continuously stirred at 150 rpm for 72 hours. Centrifuging was carried out at 9000 rpm for 15 minutes to extract the RuOH /fungi mixture obtained from the solution after 72 hours. The obtained $\text{Ru}(\text{OH})_3$ /fungi structure was washed three times with distilled water and ethanol, and centrifuged under the same conditions. As a result, the metal-precipitated biological material was collected. The resulting precipitate was then dried in a vacuum oven at 60°C for 12 hours. The dried material was subjected to heat treatment in a tube furnace over a linear temperature gradient at the temperature values needed to obtain the desired metal oxide phase. After heat treatment was performed appropriate to the desired phase, the material was placed in a Glove Box. Then, 75% of the active material, i.e. metal oxide-precipitated biological material, 20% Acetylene Black and 5% PTFE was weighed out and put in a Zr_2O_3 mortar and then ground for about 1 hour to form supercapacitor electrodes. Approximately 5 mg was weighed out from the ground material and placed on Ni Foam that had been previously prepared, and this was then used as a current collector by exposing it to 10 MPa of pressure to produce a supercapacitor electrode. This formed the study electrode whose capacitive properties were to be examined. Electrochemical measurements were performed using a 6 M KOH solution. The electrochemical cell where the measurements were made consisted of the working electrode, a platinum electrode and an Ag/AgCl reference electrode. The cyclic voltammetry (CV), charge–discharge and electrochemical impedance spectroscopy (EIS) measurements of the electrode obtained were performed using a Gamry Reference 3000

potentiostat/galvanostat/ZRA instrument. The surface properties and thermogravimetric analysis of the RuO₂/fungi microtubes were investigated using field emission scanning electron microscopy (JEOL JSM-7001F) and a thermogravimetric analyzer (Shimadzu TGA-50), respectively. The BET surface area, average pore diameter and pore volume of the RuO₂/fungi microtubes were determined using a Micromeritics Gemini VII 2390t instrument.

3. Results and Discussion

Figure 1 shows the comparison of TGA analyses of pure fungi and Ru-precipitated fungi. The mass loss of about 6.6% from room temperature to 150°C is due to the removal of water in the samples. In the TGA analysis of the Ru-precipitated fungi, a 48.55% mass loss between 200°C and 375°C is considered to be due to condensation reactions indicating rapid removal of water and ethanol from the structure. In the temperature range from 100°C to 800°C, hyphal tends to be continuously deteriorated, and also, O₂ and H₂O continuously move away from the Ru(OH)₃ structure.

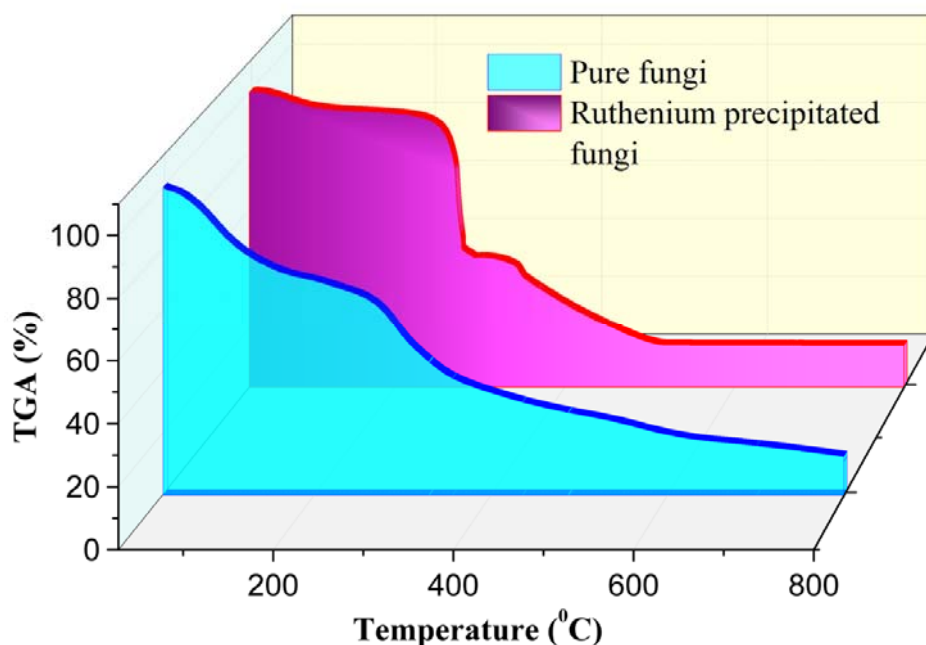
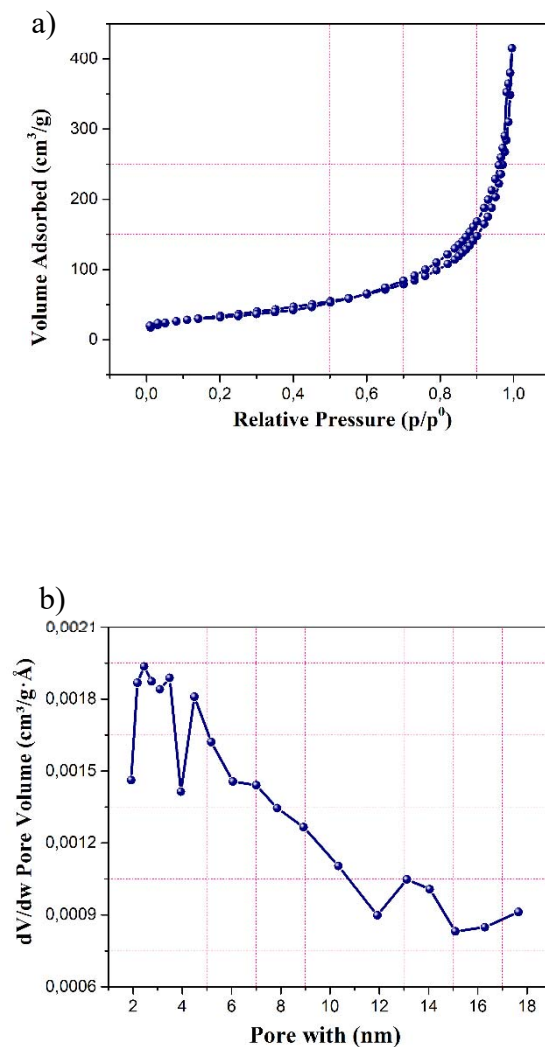


Figure 1. TGA analysis for pure fungi and metal-precipitated fungi

The total mass loss at temperatures up to 500°C in Ru-precipitated hyphal was 84%. No significant mass loss was observed in the RuO₂/fungi structure after this temperature. On the other hand, the metal non-precipitated fungi exhibited a continuous mass loss from 50°C to 750°C. This continuous mass loss is due to the degradation of water, ethanol, protein and similar substances in the biological material.

Figure 2 shows the N₂ adsorption–desorption isotherm, BJH pore diameter distribution and BET surface area change curve as a function of the temperature of the heat treatment of the metal-precipitated biological material.



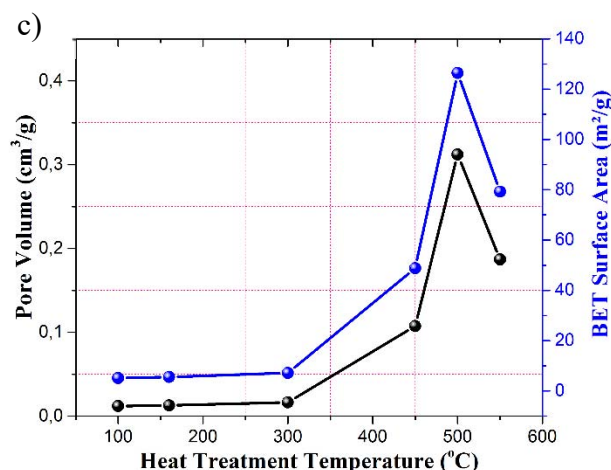
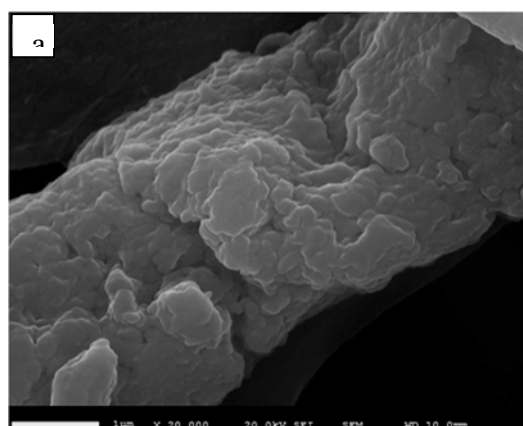


Figure 2. a) Nitrogen adsorption isotherm of nanostructured RuO₂ materials b) Pore size distribution of RuO₂ nanostructures c) BET surface area and pore volume as a function of heat treatment temperature

For the samples heat treated at different temperatures, the BET surface area measurement showed the highest surface area (126.41 m²/g) was obtained in the sample heat treated at 500°C. Also, in the sample heat treated at this temperature, the average pore diameter was around 9.8 nm with pores ranging from about 1.9 nm to 17.6 nm. The BET surface area increases up to 500°C in direct proportion to temperature and then decreases after 500°C, coincides with the TGA measurements shown in Figure 1. In accordance with this result, the sample heat treated at 500°C was used for the RuO₂/fungi electrode material. Figures 3(a-b) show SEM images of metal-precipitated fungi at different magnifications while Figures 3(c-d) show SEM images of metal-precipitated and heat treated fungi at 500°C for different magnifications. It was determined from the SEM images of metal precipitated without heat treatment of the sample that the lengths of hyphal were considerably larger (10-30 μm) and their diameter was between approximately 2 to 3 μm. Moreover, the presence of precipitated metal oxide was determined from SEM images and the surface was not too rough.



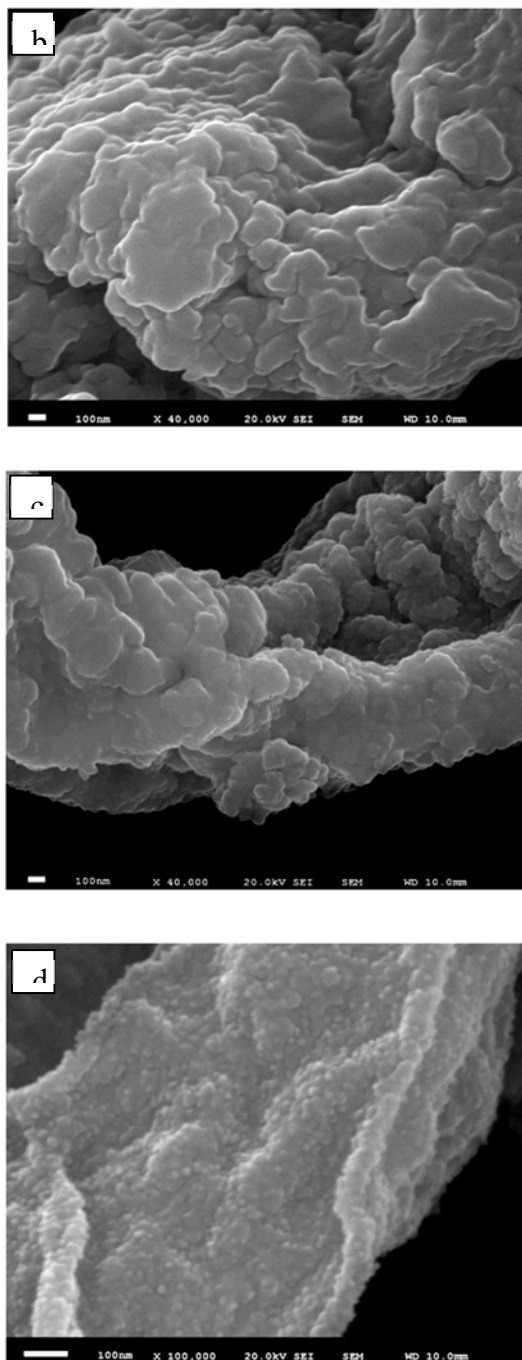


Figure 3. SEM images at different magnifications: **a-b)** chemically metal-precipitated fungi **c-d)** nanostructured RuO₂ sample after annealing process at 500°C

After heat treatment, the diameters of hyphal decreased down to 1.5 μm and the metal oxide layer around hyphal became evident and was very rough. This observation completely supported BET measurements. Figure 4 shows an EDX analysis of

precipitated metal and heat treated samples. As a result of EDX analysis, the presence of RuO₂ layer was determined on the fungi.

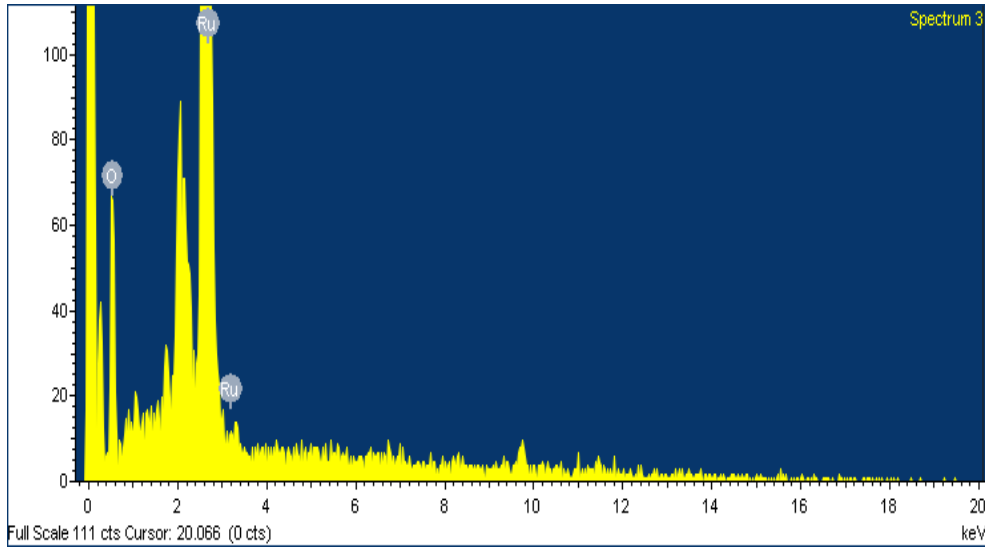


Figure 4. EDX spectrum and image of nanostructured RuO₂/fungi sample after an annealing process at 500°C

Figure 5 shows the cyclic voltammetry (CV) measurements of the electrode obtained from RuO₂-precipitated fungi performed over a potential range from 0.1 to –1 V at different scan rates, and it shows the specific capacitance change curve as a function of scan rate. CV measurements for the RuO₂/fungi electrode at different rates produced a rectangular shape, indicating better supercapacitive characteristics. The specific capacitance of the RuO₂/fungi electrode was calculated using Equation 1:

$$C_s = \frac{\int I dV}{s \times \Delta V \times m} \quad (1)$$

where I is current, s is the scan rate, ΔV is the potential range over which CV measurements were taken and m is the mass of active material. The specific capacitance value obtained using Equation 1 exhibited a very high value of 1055.7 F/g at a scan rate of 1 mV/s. This value decreased with increasing scan rate.

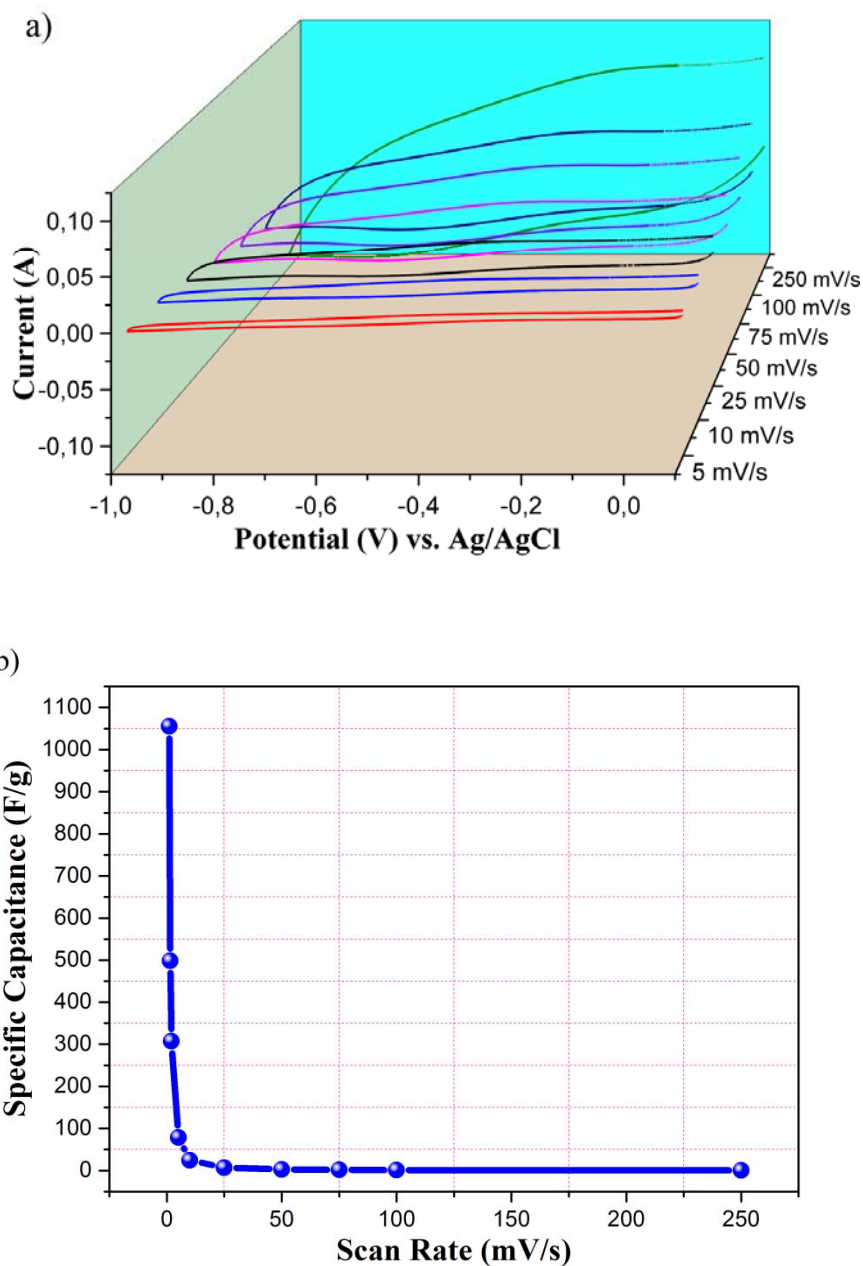


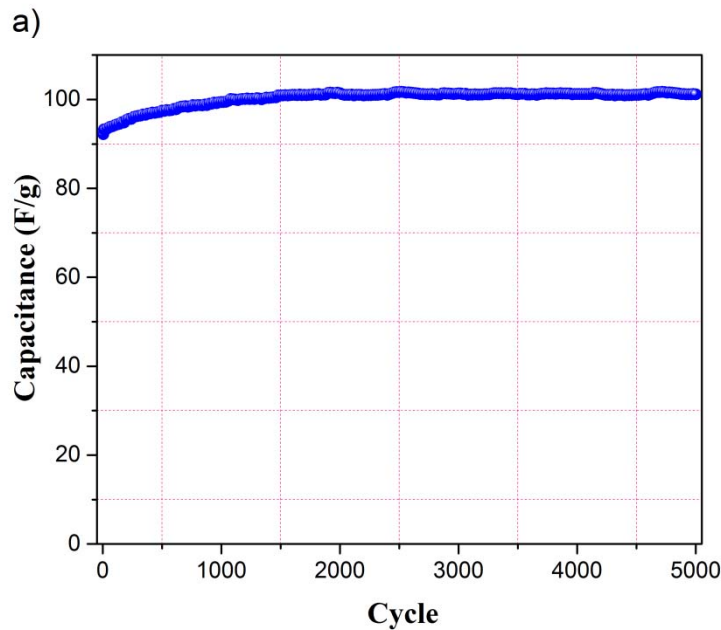
Figure 5. a) CV curves for RuO₂/fungi electrodes at different scan rates b) Specific capacitance as a function of the scan rate

The capacitive properties of the RuO₂/fungi supercapacitor electrode was investigated with a 5000 cycle charge–discharge experiment (Figure 6). The characteristic of the charge–discharge curve is its triangular shape. This configuration is desirable in supercapacitor studies because the triangular shape of the charge–discharge curve indicates good reaction reversibility. Moreover, this configuration gives more

accurate results in calculating the electrode capacitance [28]. The electrode obtained in this study showed supercapacitor behavior. Figure 6 shows the capacitance change of the RuO₂/fungi electrode calculated using Equation 2, depending on the number of cycles and the first ten charge–discharge curves of the electrode obtained at a constant current of 0.7 A/g.

$$C_s = \frac{I \times \Delta t}{m \times \Delta V} \quad (2)$$

where I is the discharge current, Δt is the discharge time, ΔV is the potential difference and m is the mass of active material present in the electrode. Using charge–discharge curves and Equation 2, capacitance values were calculated for 5000 cycles. For the first 1200 cycles, the capacitance value increased from 92 F/g to 101 F/g and remained constant for successive cycles. During the measurements, the active material on the electrode peeled over time and the active mass of the electrode decreased. The decrease in the active mass increased the capacitance. The specific capacitance value obtained from the charge/discharge tests is in accordance with the CV obtained at 5 mV/s.



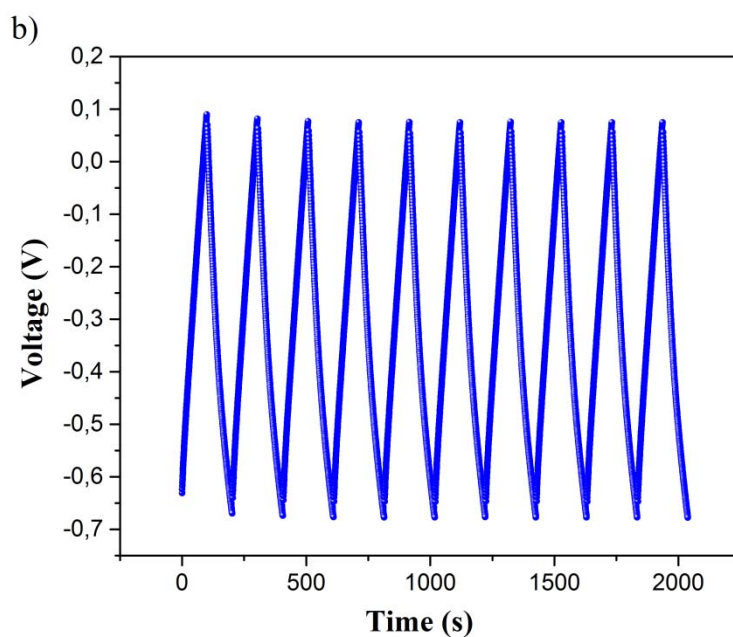


Figure 6. a) The variation of specific capacitance as a function of the number of cycles for the RuO₂/fungi electrode **b)** the ten cycle charge–discharge curves

Figure 7 shows the electrochemical impedance measurements of the RuO₂/fungi electrode obtained at 6 M of KOH for different numbers of cycles. The measurement indicated that the contact resistance between the electrolyte and RuO₂/fungi electrode did not considerably change during 5000 cycles. This phenomenon reveals that charge transfer can be achieved more easily with good electrical conductivity between the electrode/electrolyte interface. Electrochemical impedance measurements were performed after the first 10, 2000 and 5000 charge–discharge measurements. The slopes of the Nyquist curves obtained from these measurements were 72.4°, 77.2° and 80.8°, respectively. That the slope in Nyquist curve increased in direct proportion to the number of cycles and reached approximately 80.8° indicates that the electrochemical capacitive characteristic of the RuO₂/fungi electrode is good.

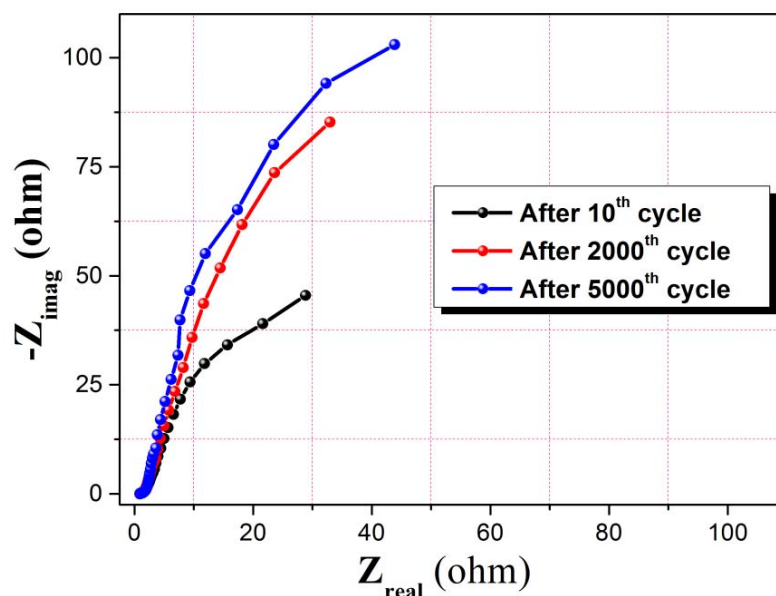


Figure 7. Nyquist plots of the RuO₂/fungi electrode after 10, 2000 and 5000 cycles at an open circuit potential in 6 M of KOH solution

4. Conclusions

RuO₂/fungi microtubes were successfully produced using a chemical precipitation method. As a result of BET surface area measurements, the highest surface area (126.41 m²/g) was obtained in the sample heat treated at 500°C. The specific capacitance value calculated from the CV curve performed at a 1 mV/s scan rate was 1055.7 F/g. The capacitance value of the RuO₂/fungi electrode calculated from the charge–discharge curve heat treated at 500°C was 101 F/g. The efficiency of the RuO₂/fungi electrode after charge–discharge measurements performed over 5000 cycles was approximately 99%. The high cost of Ruthenium in supercapacitor studies is a disadvantage, while using hyphal as a bio-substrate can eliminate this drawback.

References

- [1] Ahn, Y.R., Song, M.Y., Jo, S.M., Park, C.R., Kim, D.Y., *Electrochemical capacitors based on electrodeposited ruthenium oxide on nanofibre substrates*, Nanotechnology, 17(12), 2865, 2006.

- [2] Patake, V.D., Lokhande, C.D., Joo, O.S., *Electrodeposited ruthenium oxide thin films for supercapacitor: Effect of surface treatments*, Appl. Surf. Sci., 255(7), 4192-4196, 2009.
- [3] Hu, C.C., Huang, Y.H., Chang, K.H., *Annealing effects on the physicochemical characteristics of hydrous ruthenium and ruthenium-iridium oxides for electrochemical supercapacitors*, J. Power Sources, 108(1-2), 117-127, 2002.
- [4] Yan, J., Wei, T., Cheng, J., Fan, Z., Zhang, M., *Preparation and electrochemical properties of lamellar MnO₂ for supercapacitors*, Mater. Res. Bull., 45(2), 210-215, 2010.
- [5] Jiang, J., Kucernak, A., *Electrochemical supercapacitor material based on manganese oxide: Preparation and characterization*, Electrochim Acta, 47(15), 2381-2386, 2002.
- [6] Atalay, F.E., Asma, D., Kaya, H., Ozbey, E., *The fabrication of metal oxide nanostructures using Deinococcus radiodurans bacteria for supercapacitor*, Materials Science in Semiconductor Processing, 38, 314-318, 2015.
- [7] Atalay, F.E., Kaya, H., Asma, D., Bingöl, A., *Helical microtubules of nanostructured cobalt oxide for electrochemical energy storage applications*, Biointerface Research in Applied Chemistry, 6(2), 1099-1103, 2016.
- [8] Patil, U.M., Salunkhe, R.R., Gurav, K.V., Lokhande, C.D., *Chemically deposited nanocrystalline NiO thin films for supercapacitor application*, Appl. Surf. Sci., 255(2), 2603-2607, 2008.
- [9] Nelson, P.A., Owen, J.R., *A high-performance supercapacitor/battery hybrid incorporating templated mesoporous electrodes*, J. Electrochem. Soc., 150(10), A1313, 2003.
- [10] Kandalkar, S.G., Gunjekar, J.L., Lokhande, C.D., *Preparation of cobalt oxide thin films and its use in supercapacitor application*, Appl. Surf. Sci., 254(17), 5540-5544, 2008.

[11] Miura, N., Oonishi, S., Rajendra Prasad, K., *Indium tin oxide/carbon composite electrode material for electrochemical supercapacitors*, *Electrochem Solid-State Lett.*, 7(8), A247, 2004.

[12] Hu, C.C., Huang, C.M., Chang, K.H., *Anodic deposition of porous vanadium oxide network with high power characteristics for pseudocapacitors*, *J. Power Sources*, 185(2), 1594-1597, 2008.

[13] da Silva, D.L., Delatorre, R.G., Pattanaik, G., Zangari, G., Figueiredo, W., Blum, R.P., et al., *Electrochemical synthesis of vanadium oxide nanofibers*, *J. Electrochem Soc.*, 155(1), E14, 2008.

[14] Zhou, X., Chen, H., Shu, D., He, C., Nan, J., *Study on the electrochemical behavior of vanadium nitride as a promising supercapacitor material*, *J. Phys. Chem. Solids*, 70(2), 495-500, 2009.

[15] Nakayama, M., Tanaka, A., Sato, Y., Tonosaki, T., Ogura, K., *Electrodeposition of manganese and molybdenum mixed oxide thin films and their charge storage properties*, *Langmuir*, 21(13), 5907-5913, 2005.

[16] Babakhani, B., Ivey, D.G., *Anodic deposition of manganese oxide electrodes with rod-like structures for application as electrochemical capacitors*, *J. Power Sources*, 195(7), 2110-2117, 2010.

[17] Zheng, J.P., Cygan, P.J., Jow, T.R., *Hydrous ruthenium oxide as an electrode material for electrochemical capacitors*, *J. Electrochem. Soc.*, 142, 2699-2703, 1995.

[18] Zheng, J.P., *Ruthenium oxide-carbon composite electrodes for electrochemical capacitors*, *Electrochem, Solid-State Lett.*, 2, 359-361, 1999.

[19] Ramani, M., Haran, B.S., White, R.E., Popov, B.N., Arsov, L., *Studies on activated carbon capacitor materials loaded with different amounts of ruthenium oxide*, *J. Power Sources*, 93, 209-214, 2001.

[20] Hu, C.C., Chen, W.C., Chang, K.H., *How to achieve maximum utilization of hydrous ruthenium oxide for supercapacitors*, *J. Electrochem. Soc.*, 151, A281-A290, 2004.

[21] Lee, Y.H., Oh, J.G., Oh, H.S., Kim, H., *Novel method for the preparation of carbon supported nano-sized amorphous ruthenium oxides for super capacitors*, *Electrochem. Commun.*, 10, 1035-1037, 2008.

[22] Atalay, F.E., Asma, D., Kaya, H., Bingol, A., Yaya, P., *Synthesis of NiO nanostructures using Cladosporium cladosporioides fungi for energy storage applications*, *Nanomaterials and Nanotechnology*, 6:28, DOI: 10.5772/63569, 2016.

[23] Fontes, A.M., Geris, R., dos Santos, A.V., Pereira, M.G., Ramalho, J.G.S., da Silva, A.F., Malta, M., *Bio-inspired Au microtubes based on morphology of filamentous fungi*, *Biomater. Sci.*, 2, 956-960, 2014.

[24] Li, Z., Chung, S.W., Nam, J.M., Ginger, D.S., Mirkin, C.A., *Living templates for the hierarchical assembly of gold nanoparticles*, *Angew. Chem. Int. Ed.*, 42, 2306-2309, 2003.

[25] Sugunan, A., Melin, P., Schnürer, J., Hilborn, J. G., Dutta, J., *Nutrition-driven assembly of colloidal nanoparticles: Growing fungi assemble gold nanoparticles as microwires*, *Adv. Mater.*, 19, 77-81, 2007.

[26] Bigall, N.C., Reitzig, M., Naumann, W., Simon, P., van Pee, K.H., Eychemüller, A., *Fungal templates for noble-metal nanoparticles and their application in catalysis*, *Angew. Chem. Int. Ed.*, 47, 7876-7879, 2008.

[27] Fakhrullin, R.F., Zamaleeva, A. I., Minullina, R. T., Konnova, S. A., Paunov, V.N., *Cyborg cells: Functionalisation of living cells with polymers and nanomaterials*, *Chem. Soc. Rev.*, 41, 4189-4206, 2012.

[28] Kampouris, D.K., Ji, X., Randviir, E.P., Banks, C.E., *A new approach for the improved interpretation of capacitance measurements for materials utilised in energy storage*, *RSC Adv.*, 5, 12782-12791, 2015.